Analog Broadband Linearization of a Q-Band Solid-State Power Amplifier Using a SiGe Linearizer RFIC with Controlled IMD Injection

Mathias P. Scharpf[#1], Burak G. Özat[#2], Benjamin Schoch[#3], Ingmar Kallfass[#4]

[#]Institute of Robust Power Semiconductor Systems (ILH), University of Stuttgart, Germany

{[1]mathias-pius.scharpf, [2]burak.oezat, [3]benjamin.schoch, [4]ingmar.kallfass}@ilh.uni-stuttgart.de

***Abstract* — This paper presents a proof-of-concept demonstration of broadband analog linearization at Q-band, in which a SiGe linearizer RF integrated circuit is used to linearize a commercial solid-state power amplifier (SHF S807C). The approach is based on the controlled generation and injection of third-order intermodulation products to compensate nonlinear distortion directly in the RF domain. A measurement-based Nelder-Mead optimization routine adjusts five DC control voltages of the LRFIC to minimize distortion at the amplifier output. The concept is validated under 32-APSK modulation at 4 GBaud (4 GHz bandwidth). Measurements yield an adjacent channel power ratio improvement of 7.7 dB (lower) and 2.4 dB (upper), a reduction in error vector magnitude from 8.49 % to 5.74 %, and a signal-to-noise ratio improvement of 3.4 dB at the optimized operating point. These results demonstrate the feasibility of controlled IMD-based analog linearization for broadband Q-band systems and highlight its potential for satellite communication transmitter architectures.**

***Keywords* — Analog predistortion (APD), Intermodulation distortion (IMD), Power amplifier linearization, Q-band, Broadband systems, SiGe BiCMOS, Satellite communications.**

I. Introduction

Millimeter-wave communication systems increasingly rely on high-order modulation schemes and wideband signals, imposing stringent linearity requirements on transmitter architectures. In Q-band systems, power amplifiers are often operated close to saturation to maximize efficiency, resulting in nonlinear distortion, spectral regrowth, and degradation of signal quality. These effects are commonly quantified using adjacent channel power ratio (ACPR) and error vector magnitude (EVM).

Digital predistortion (DPD) is widely used to compensate nonlinearities at lower frequencies and small bandwidths [1]. However, its application at millimeter-wave frequencies is challenging due to large signal bandwidths, hardware complexity, and power consumption. Achieving linearization for multi-GHz bandwidth signals requires wideband feedback paths and high-speed data converters, resulting in significant system overhead [2].

Analog predistortion (APD) techniques offer an alternative by operating directly in the RF domain, avoiding high-speed digital processing. However, conventional APD approaches often suffer from limited control over the amplitude, phase, and delay of the generated intermodulation distortion (IMD) products, which becomes critical under broadband conditions [3]. Controlled IMD injection has emerged as a promising approach, enabling independent tuning of distortion components [4].

In this work, a transmitter-level proof-of-concept demonstration is presented in which the linearizer RF integrated circuit (LRFIC) linearizes an external solid-state power amplifier (SHF S807C) under broadband 32-APSK excitation with 4 GHz bandwidth. In contrast to prior work [4], which validated self-linearization of the LRFIC itself, this work demonstrates linearization of a cascaded external amplifier, confirming the broader applicability of the concept. The underlying circuit implementation of the LRFIC is reported separately.

II. Transmitter-Level Linearization Concept

The proposed approach is based on the controlled generation and injection of third-order intermodulation (IM3) products to compensate nonlinear distortion directly in the RF domain. As illustrated in Fig. 1, the input signal is split into a linear branch (LB), which carries the fundamental signal components, and a nonlinear branch (NLB), which generates controllable IM3 components. By adjusting the amplitude, phase, and delay of the NLB output, destructive interference with the distortion generated by a subsequent nonlinear device is achieved.

In contrast to conventional APD approaches, the proposed concept enables independent control of IM3 amplitude and phase, which is particularly important for broadband signals and for adapting to different amplifier characteristics. The LRFIC is implemented in IHP 130 nm SiGe BiCMOS technology, covering 37.5–42.5 GHz. It provides 0 to $+5$ dBm output power for a -20 dBm nominal input power.

In this work, an SHF S807C broadband solid-state amplifier is used as the device under test (DUT). The amplifier operates from 70 kHz to 55 GHz and enters saturation above an input power level of approximately -8 dBm, with a maximum output power of 18.5 dBm.

III. Experimental Setup

A. Measurement Setup

The measurement setup is illustrated in Fig. 2. A Keysight PNA-X (N5244B) is used for signal routing and acquisition. A broadband 32-APSK signal is generated by an external

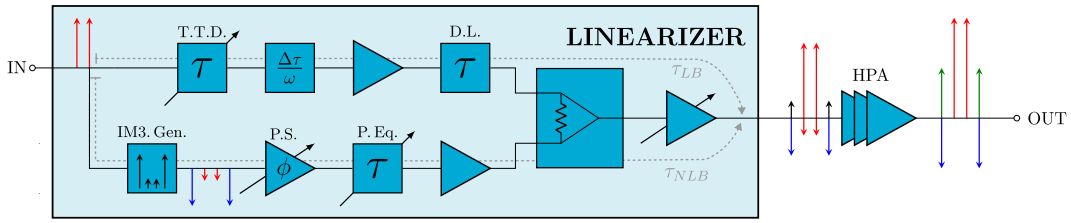

Fig. 1. Simplified block diagram of the linearizer RFIC. The LB (top) forwards the fundamental signal via a tunable true-time delay and a fixed delay line. The NLB (bottom) generates IM3 components using an IM3 generator, a vector modulator for independent amplitude (0–15 dB) and phase (0–360°) control, and a tunable phase equalizer. Both branches are recombined and followed by a variable-gain output stage. The cascaded SHF S807C (HPA) is connected at the LRFIC output.

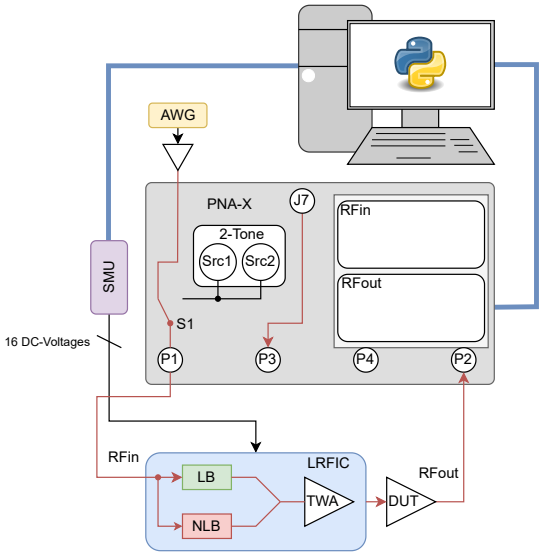

Fig. 2. Laboratory measurement setup. The LRFIC is operated on a wafer prober; the SHF S807C (DUT) is connected at the LRFIC output. A Python-based optimization algorithm adjusts the LRFIC control voltages based on EVM and ACPR measured at the DUT output.

arbitrary waveform generator (AWG) and amplified by a highly linear driver amplifier to compensate for cable and probe losses. The LRFIC is mounted on a wafer prober and contacted via RF probes. DC control voltages are supplied by a source measurement unit (SMU). The SHF S807C DUT is connected directly at the LRFIC output, and the combined output signal is acquired by the PNA-X for analysis.

The LRFIC and DUT are operated as a cascaded system. The LRFIC input power is set to -25 dBm. With a system gain of approximately 22 dB, the resulting DUT input power is -3 dBm, placing the DUT approximately 5 dB into saturation. This operating point is chosen to introduce clearly measurable distortion while remaining within a regime where the LRFIC can provide effective IM3 compensation. To compare linearized and non-linearized operation, the NLB can be selectively disabled, allowing direct observation of the uncompensated distortion. To exclude a change of operating point as the cause of any improvement, a constant output power constraint is enforced at the DUT output throughout the optimization.

A 32-APSK signal at 4 GBaud (approximately 4 GHz

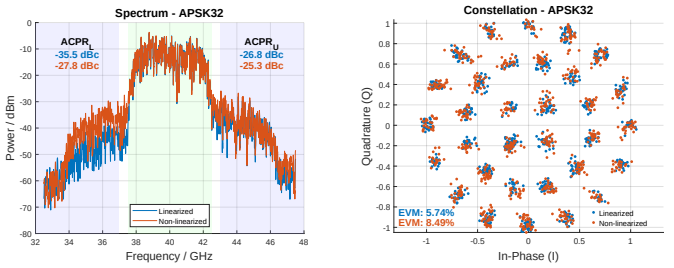

(a) (b)

Fig. 3. Measured output spectra (a) and 32-APSK constellation diagrams (b) without and with linearization under 32-APSK excitation (4 GBaud, -25 dBm LRFIC input). The EVM is reduced from 8.49 % to 5.74 %.

bandwidth) is used for evaluation. All results are obtained at the optimized operating point, with the output power fixed at 13.9 dBm.

B. *Measurement-Based Optimization*

The LRFIC is tuned using a fully automated measurement-based optimization routine implemented in Python. The Nelder-Mead algorithm is employed due to its robustness against measurement noise, gradient-free operation, and suitability for low-dimensional parameter spaces.

The optimizer controls five DC voltages supplied via the SMU: one voltage sets the IM3 purity as a function of input power level, while four voltages tune the amplitude and phase of the IM3 components via the vector modulator in the NLB. Starting from a predefined set of default bias conditions, the control voltages are iteratively updated. After each update, EVM and ACPR are measured at the DUT output using vector signal analysis (VSA) software on the PNA-X, and the results are fed back to the optimizer. The loop terminates when no further improvement is observed over a predefined number of iterations, and the best-performing control voltage set is selected as the final operating point.

IV. Broadband Linearization Results

The linearization performance of the cascaded LRFIC + SHF S807C system is evaluated under 32-APSK modulation at 4 GBaud. Fig. 3a shows the measured output spectra for the non-linearized and linearized cases at equal output power (13.9 dBm). Without linearization, the system exhibits spectral regrowth with an ACPR of -28.8 dBc (lower) and -25.3 dBc (upper).

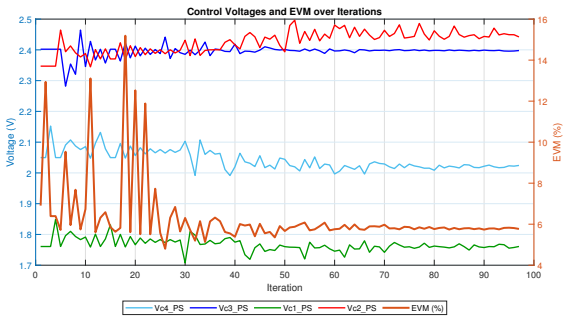

Fig. 4. Convergence behavior of the optimization routine showing four control voltages and EVM over iterations. The fifth control voltage (IM3 purity) is omitted as it remains nearly constant throughout.

By enabling the NLB and optimizing the control voltages, the ACPR improves to $-36.5\,\mathrm{dBc}$ (lower) and $-27.7\,\mathrm{dBc}$ (upper), corresponding to an improvement of 7.7 dB and 2.4 dB for the lower and upper adjacent channels, respectively. The asymmetry in the ACPR improvement arises from the optimization objective: the optimizer minimizes EVM rather than ACPR directly, which may favor cancellation in one sideband over the other. Under broadband excitation with 4 GHz bandwidth, distortion components exhibit strong frequency-dependent behavior, requiring precise alignment of IM3 amplitude and phase across the full signal bandwidth.

The impact on in-band signal quality is shown in Fig. 3b. The EVM is reduced from 8.49 % to 5.74 %, and the signal-to-noise ratio (SNR) improves from 19.4 dB to 22.8 dB, corresponding to an SNR gain of 3.4 dB. This confirms that the injected IM3 components compensate the nonlinear behavior of the DUT not only in the adjacent channels but also within the signal band.

The convergence behavior of the optimization is shown in Fig. 4. During an initial exploration phase, pronounced fluctuations are observed, during which the EVM temporarily degrades. As the optimization progresses, the control voltages converge to stable values and the EVM decreases consistently. A correlation between EVM and $V_{c1,2}$ is observed, which can be attributed to its role as the primary control voltage of the vector modulator in the NLB, governing the amplitude and phase alignment of the injected IM3 components relative to the fundamental signal. After approximately 30 iterations, the EVM reaches a plateau, indicating convergence. Note that only four of the five control voltages are shown in Fig. 4; the fifth voltage, which sets the IM3 purity as a function of input power level, remains nearly constant throughout the optimization, consistent with the enforced output power constraint. The improvement is reproducible across repeated measurements at the optimized operating point.

V. Comparison and Discussion

Table 1 summarizes representative analog and digital predistortion approaches at microwave and millimeter-wave frequencies, highlighting trade-offs between linearization performance, bandwidth, and operating frequency.

DPD achieves high linearization performance, typically exceeding 20 dB ACPR improvement [1], [2]. However, these approaches require wideband feedback paths and high-speed data converters, making them increasingly impractical for multi-GHz bandwidths at millimeter-wave frequencies.

Existing APD implementations either target sub-6 GHz frequency ranges [5], are tailored to specific amplifier characteristics [3], or are limited to narrowband conditions. As shown in Table 1, no prior work demonstrates APD at Q-band with multi-GHz bandwidth under spectrally efficient modulated excitation for an external power amplifier. The presented work directly addresses this gap.

The achieved ACPR improvement must be interpreted in the context of the experimental setup. The LRFIC is optimized for a nominal input power of $-20\,\mathrm{dBm}$, while in this experiment it is operated at $-25\,\mathrm{dBm}$ to avoid driving the DUT too deeply into compression. Consequently, the LRFIC operates below its optimal design point, which limits the available IM3 injection power. Furthermore, the SHF S807C is not the primary target amplifier for this linearizer – it serves as an accessible proof-of-concept DUT. In satellite communication systems, where dedicated HPAs are driven deep into compression to maximize power-added efficiency (PAE), significantly larger linearization gains are expected.

The Nelder-Mead optimization converges robustly despite measurement fluctuations, reaching a stable operating point after approximately 30 iterations (Fig. 4). The consistent reduction in EVM confirms that the algorithm is well-suited for practical, model-free tuning of the LRFIC under realistic operating conditions. The high degree of tunability of the LRFIC makes the concept readily extendable to other amplifier types, positioning it as a scalable building block for next-generation wideband Q-band transmitter architectures.

VI. Conclusion

This work presents a proof-of-concept demonstration of broadband analog linearization at Q-band, in which a SiGe LRFIC linearizes a commercial solid-state power amplifier (SHF S807C) under 32-APSK modulated excitation with 4 GHz bandwidth. A measurement-based Nelder-Mead optimization routine controlling five DC bias voltages enables robust, automated tuning of the LRFIC under realistic operating conditions.

Evaluated at a fixed output power of 13.9 dBm, the approach yields an ACPR improvement of 7.7 dB (lower) and 2.4 dB (upper), an EVM reduction from 8.49 % to 5.74 %, and an SNR improvement of 3.4 dB. The consistent improvement across both in-band and out-of-band metrics confirms that the linearization mechanism operates effectively over the full signal bandwidth.

The demonstrated concept is not limited to the chosen DUT and is inherently scalable to high-power amplifiers in satellite communication payloads, where larger linearization gains are expected under stronger compression. This establishes controlled IMD injection using an integrated, tunable SiGe LRFIC as a viable building block for flexible broadband

Table 1. Comparison of state-of-the-art analog and digital predistortion techniques.

Work / Year	**Type**	f_c **(GHz)**	**BW (GHz)**	**Modulation**	**ΔACPR (dB)**	**Remark**
[1] '20	DPD	25–63	0.4	OFDM	20–30	Narrowband, high complexity
[2] '21	DPD	28	0.4	5G NR	>10	Phased-array system
[3] '25	APD	2–3	0.08	OFDM	7.3–9.6	Sub-6 GHz, PA-specific
[5] '15	APD	<40	0.4	WiFi OFDM	5–10	Broadband RoF system
[6] '18	APD	2.4	<0.02	WCDMA	13	IMD3 reduction
This work	**APD**	**40**	**4**	**32-APSK**	**7.7 / 2.4**	**Q-band mmWave**

analog predistortion in next-generation Q-band transmitter architectures.

ACKNOWLEDGMENT

The authors gratefully acknowledge the funding and support provided by the German Aerospace Center (DLR) through the project "Enhanced Self-Calibrating Amplifier Component for Space (ESCALAS)" under contract number 50RK2320, as well as the technical support provided by TESAT Spacecom GmbH & Co. KG.

REFERENCES

[1] I. Jaffri, A. B. Ayed, A. M. Darwish, P. Mitran, and S. Boumaiza, "Novel baseband equivalent model for digital predistortion of wideband frequency-multiplier-based millimeter wave sources," *IEEE Transactions on Microwave Theory and Techniques*, vol. 68, no. 9, pp. 3942–3957, 2020.

[2] N. Tervo, B. Khan, O. Kursu, J. P. Aikio, M. Jokinen, M. E. Leinonen, M. Juntti, T. Rahkonen, and A. Pärssinen, "Digital predistortion of phased-array transmitter with shared feedback and far-field calibration," *IEEE Transactions on Microwave Theory and Techniques*, vol. 69, no. 1, pp. 1000–1015, 2021.

[3] A. Pitt, M. Beach, and T. Cappello, "An analog gain inflection predistorter for combined back-off efficiency and linearity with doherty power amplifiers," *IEEE Transactions on Microwave Theory and Techniques*, vol. 73, no. 1, pp. 167–179, 2025.

[4] S. Koch, M. Schick, A. Fischer, C. Bohn, M. Jutzi, L. Baumgärtner, A. Scharpf, J. Schlipf, J. S. Reckter, and B. Klingenberg, "A broadband analog linearizer for ka-band satellite communication utilizing imd self-alignment based on radiation hard sige-hbt," in *2025 20th European Microwave Integrated Circuits Conference (EuMIC)*, 2025, pp. 17–20.

[5] R. Zhu, Z. Xuan, Y. Zhang, X. Zhang, and D. Shen, "Novel broadband analog predistortion circuit for radio-over-fiber systems," in *2015 IEEE MTT-S International Microwave Symposium*, 2015, pp. 1–4.

[6] Q. Cai, W. Che, K. Ma, and M. Zhang, "A simplified transistor-based analog predistorter for a gan power amplifier," *IEEE Transactions on Circuits and Systems II: Express Briefs*, vol. 65, no. 3, pp. 326–330, 2018.